

Sociedade & Natureza

ISSN: 1982-4513

Universidade Federal de Uberlândia, Instituto de Geografia, Programa de Pós-Graduação em Geografia

Guilherme, Adriano Pereira; Biudes, Marcelo Sacardi;
Mota, Deniz dos Santos; Musis, Carlo Ralph De
Relationship between soil cover type and surface temperature
Sociedade & Natureza, vol. 32, 2020, pp. 515-525
Universidade Federal de Uberlândia, Instituto de Geografia, Programa de Pós-Graduação em Geografia

DOI: https://doi.org/10.14393/SN-v32-2020-47462

Available in: https://www.redalyc.org/articulo.oa?id=321364988039



Complete issue

More information about this article

Journal's webpage in redalyc.org



Scientific Information System Redalyc

Network of Scientific Journals from Latin America and the Caribbean, Spain and Portugal

Project academic non-profit, developed under the open access initiative



Relationship between soil cover type and surface temperature

Adriano Pereira Guilherme¹ Marcelo Sacardi Biudes² Deniz dos Santos Mota³ Carlo Ralph De Musis⁴

Keywords:

Remote sensing. Temperature mapping. Urbanization. Coari - AM

Abstract

Microclimates are sensitive to surface cover type. Changes in vegetation cover modify energy distribution patterns, strongly impacting essential variables such as temperature and relative humidity. Regions with high vegetal cover density channel much of the energy through evapotranspiration, thus promoting a tremendous thermo-hydroregulating effect on the environment. The mapping of climatological variables through remote sensing and geoprocessing techniques can help in dimensioning this phenomenon and has become a popular technique due to the high availability of data from orbital satellite images and lower cost. This work uses images from the Landsat 8 satellite from the United States Geological Survey to map vegetation, urbanization and surface temperature in the urban area of Coari, Amazonas - Brazil in two distinct periods (2015 and 2017), seeking a quantitative evaluation of the influence of vegetation and urbanization on the values of this temperature. This study also attempts to estimate the importance of the atmospheric correction for this estimate and the difference in general climate conditions between the dates. The research shows that there is a considerable influence of vegetation on temperature control, despite higher reflective capacity (albedo) of urbanized areas. The urbanized regions showed temperatures up to 7°C higher than densely vegetated regions. Atmospheric correction in the temperature estimation is crucial, otherwise values can be severely underestimated. Temperatures in 2015 were substantially higher on soil regions, but lower in the water bodies, which is counterintuitive. Finally, this study may suggest a greater commitment of the public power in the promotion of policies aimed at the afforestation and vegetation of urban centers.

¹ Universidade Federal do Amazonas, Coari, Amazonas, Brasil. adrianopgpg@gmail.com

² Universidade Federal de Mato Grosso, Cuiabá, Mato Grosso, Brasil. marcelo@fisica.ufmt.br

³ Universidade Federal do Amazonas, Manaus, Amazonas, Brasil. dmotaufam@gmail.com

⁴ Universidade de Cuiabá, Cuiabá, Mato Grosso, Brasil. carlo.demusis@gmail.com

INTRODUCTION

The Amazon rainforest provides various environmental services, the most important ones being maintaining biodiversity, water cycling, and a large capacity to store carbon. However, deforestation has increased considerably in the last decades in the region (FEARNSIDE, 2006). Although deforestation is much smaller in the interior of the legal Amazon, being more restricted to the southern and western Amazon states (FERREIRA et al., 2005), it is essential to recognize the local impacts of urban expansion in the region, which has advanced considerably in recent decades (MOURÃO, 2007; PAVÃO et al., 2017). The municipality of Coari, Amazonas, Brazil, has gone through a period of rapid expansion. The number of inhabitants went from 38 thousand in 1992 to more than 78 thousand in (IBGE, 2011). growth 2010This has significantly transformed land use (GUILHERME et al., 2016), partly due to the prospecting and exploration of oil and gas, but also due to livestock and extractive expansion, which resulted in the disfigurement of the original forest matrix.

The regional microclimate is sensitive to the surface cover and associated with the usage of available energy for heating the soil and atmosphere (sensitive heat) and evapotranspiration (latent heat). Changes in the vegetation cover modify the distribution patterns of the available energy, changing temperature and relative air humidity. Regions with a high density of vegetation cover dissipates most of the solar energy through evapotranspiration, which acts as a thermohydroregulator ofenvironment the (MEDEIROS et al., 2005; VAREJÃO-SILVA, 2006; BIUDES et al., 2015). The effect of urbanization in the Amazon region on the little-known surface temperature isa phenomenon.

Surface data collection techniques from sensors in orbital satellites have become increasingly common. These techniques allows us to monitor several meteorological and environmental phenomena on the surface, such as weather forecasting, resource management, and management and better understand the effect of human activity on climate change (CHEN et al., 2006; ALLEN et al., 2007; SHALABY; TATEISHI, 2007). The main advantages of remote sensing when compared to measurements in loco are lower cost, smaller larger operational difficulty, amount

available data, and more extensive spatial information, which becomes especially crucial in geographically heterogeneous regions (PAVÃO et al., 2017). The research was done using data from the Landsat 8 - the most recent satellite in activity in the Landsat program (started in 1972), of the United States Geological Survey (USGS). It has excellent spatial and temporal resolutions and free data availability.

Landsat 8 images can be used to obtain critical physical measurements after processing using specific mathematical models. As an example, we can use the land surface temperature (LST), surface albedo (solar radiation reflection coefficient of the surface) and vegetation indexes (NDVI, SAVI, IAF and coverage fraction vegetation (Fc) to quantitatively estimate vegetation and biomass in a given region.

Several studies have shown that the surface temperature in urban areas is significantly higher than in vegetated areas (GARTLAND, 2010), which is of critical importance in regions with naturally hot climates, such as the Amazon. High temperatures have tremendous negative impact, affecting people in different ways, causing occasional minor discomforts and damaging health (thermal stress and reduced air quality, for example) and even cognitive ability (GAOUA et al., 2011; MCMORRIS et al., 2006). Additionally, high temperature have a negative economic impact for the population due to increased demand for electricity and reduced productivity (ZANDER et al., 2015; STERN, 2013; TAWATSUPA et al, 2013; TAMM et al, 2014; DARCAN; GUNEY, 2008; MADER et al., 2010).

Thus, the objective of our study is to evaluate the spatial distribution of surface temperature and vegetation in the urban area of Coari, Amazonas - Brazil, and its surroundings. We also assessed the importance of atmospheric correction of the surface temperature to compare it on two dates, being one of them a year of strong El Niño (2015). The results can bring about greater awareness for residents of urban centers and even a new orientation to the public system, in the sense of promoting policies for the increase and preservation of vegetated areas in the cities.

MATERIAL AND METHODS

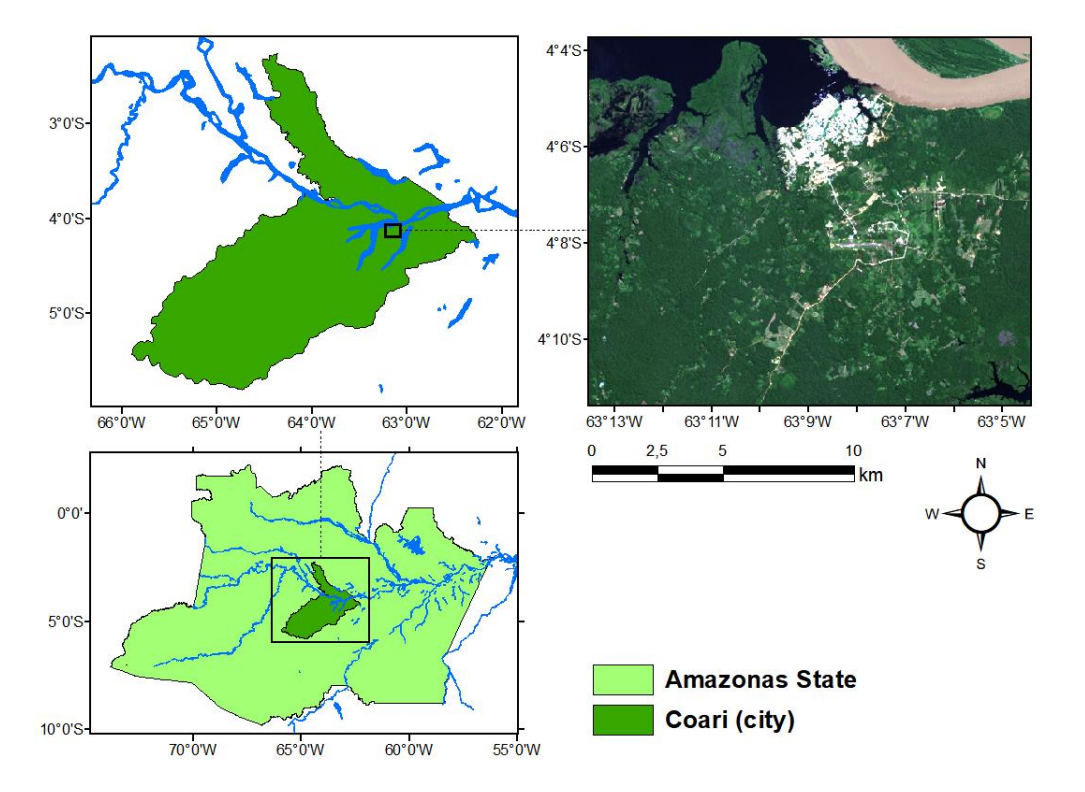
Study Area Description

This study analyzes the urban area and its

surroundings in the municipality of Coari, Amazonas - Brazil (Fig. 1). The study area is in the subarea regionaly known as the Médio Solimões (AB'SABER, 2010), at approximate 4° S e 63° W. The region's climate is warm and

humid equatorial. The urban area is located next to the Solimões River between the Coari and Mamiá Lakes, with an average altitude of 46 m (IBGE, 2011).

Figure 1 - Location of the study area in the municipality of Coari, Amazonas, Brazil.



Source: Org. by the Author, 2020.

Satellite Images Description

The Landsat 8 satellite was launched on 11 February 2013 and has two sensing instruments, the Operational Land Imager (OLI) and the Thermal Infrared Sensor (TIRS). OLI has nine spectral bands ranging from 430 to 1380 nm, and TIRS has two bands of thermal infrared from 10600 to 12510 nm. Each image is formed by an 11-layer raster image, in the form of a 185 km long square (USGS, 2016).

The images used correspond to path 233 and row 63 of Landsat 8 on 08/24/2015 and (local 06/26/2017, at 10:25am time), downloaded from the Global Visualization Viewer (GLOVIS, 2019) of the United States Geological Survey (USGS). Surface reflectance's corrected for atmospheric effects were obtained from the USGS (ESPA, 2019). The criterion for image selection used was the almost total absence of clouds. Each spectral band has its calibration coefficients, available in a text file (metadata) with the downloaded

image.

Images Processing

The spectral radiance of each band was calculated by Equation (1).

$$L_{\lambda(TOA)} = M_L Q_{cal} + A_L \tag{1}$$

where $L_{\lambda(TOA)}$ is the spectral radiance at the top of the atmosphere (W/m⁻² srad⁻¹ µm⁻¹) M_L and A_L are tabulated rescheduling parameters for calculating radiance and Q_{cal} is the calibrated and quantized digital number of the image.

The surface reflectance in each band is symbolized by ρ_{λ} and has already been corrected for the effect of the atmosphere and elevation of the Sun. The quantitative estimation of vegetation was done using the vegetation indices. The Normalized Difference Vegetation Index (NDVI) was calculated by equation (2) to identify the density of green

vegetation and its spatial distribution in the study area (TUCKER, 1979).

$$NDVI = \frac{\rho_5 - \rho_4}{\rho_5 + \rho_4} \tag{2}$$

where ρ_4 and ρ_5 are the surface reflectances of the band 4 and 5 of the Landsat 8, which correspond to the red and near-infrared bands, respectively. NDVI can range from -1 to 1 and indicate the vegetation cover of the study area. The higher the index value, the greater the presence of vegetation. The reason for using these specific bands is due to the higher absorbance in the red band and the greater reflectance in the near-infrared band by the vegetation cover. Another index that may be more appropriate to help in the comparison of the surface temperature images is the vegetation fraction (Fc), calculated by equation (3) (CARLSON; RIPLEY, 1997).

$$Fc = \left(\frac{NDVI - NDVI_{min}}{NDVI_{max} - NDVI_{min}}\right)^{2} \tag{3}$$

where $NDVI_{min}$ e $NDVI_{max}$ are the minimum and maximum NDVI of the image, respectively.

The surface temperature must be corrected for the effects of the atmosphere and the emissivity of the surface since the temperature without corrections is significantly underestimated (PRICE, 1983). Thus, the corrected thermal radiance is equivalent to that of a blackbody at a given temperature. The atmospheric correction of the temperature was carried out, according to BARSI et al. (2003).

$$L_{\lambda} = \frac{L_{\lambda(TOA)} - L_u - (1 - \varepsilon)L_d}{\varepsilon\tau} \tag{4}$$

where L_{λ} is the corrected thermal radiance, ε is the surface emissivity, L_u is the upwelling radiance, L_d is the downwelling radiance, and τ is the thermal atmospheric transmissivity. The last three parameters can be obtained by the algorithm developed by NASA's Goddard Space Flight Center (GSFC, 2019). The emissivity of the surface was calculated by equation (5) (VALOR; CASELLES, 1996).

$$\varepsilon = \varepsilon_v Fc + \varepsilon_g (1 - Fc)(1 - 0.74Fc) + 1.7372Fc(1 - Fc)$$
(5)

where ε_v vegetation emissivity ($\varepsilon_v = 0.985$) and ε_q is the soil emissivity ($\varepsilon_q = 0.960$).

The surface temperature (LST; °C) was calculated by equation (6), which is based on the Planck equation.

$$LST = \frac{K_2}{\ln\left(\frac{K_1}{L_2} + 1\right)} - 273.15\tag{6}$$

where K_1 e K_2 are calibration constants provided in the metadata file.

The surface albedo (a), which synthetically consists of the reflective power of a surface, was calculated according to the procedure described by Silva (2016). Because the forest has high radiation absorption power, albedo can be an indicator of built-up areas or exposed soil. The Normalized Difference Built-up Index (NBDI) was calculated by equation (7) (ALHAWITI; MITSOVA, 2016).

$$NDBI = \frac{\rho_6 - \rho_5}{\rho_6 + \rho_5} \tag{7}$$

Data Analysis

With the LST histograms, we were able to calculate the average temperatures in each of the regions and form a preliminary idea of the impact of vegetation on these values. A supervised classification of land use (with previous training for the algorithm) to assist in the visual comparison of the surface temperature was also carried out.

A comparison between Bright Temperature (BT) (Temperature estimated without correction) and LST was made to measure the importance of correcting the effect of the atmosphere in the surface temperature estimates.

Finally, in order not to base our discussions solely on visual impressions, scatter plots between the stretched values of α, LST, NDVI, and NDBI were created and 1600 points were defined at random in the study area to estimate the values of each image (Fig. 2). The sample points related to the bodies of water were discarded, which reduced the sample to 1376 to ints.

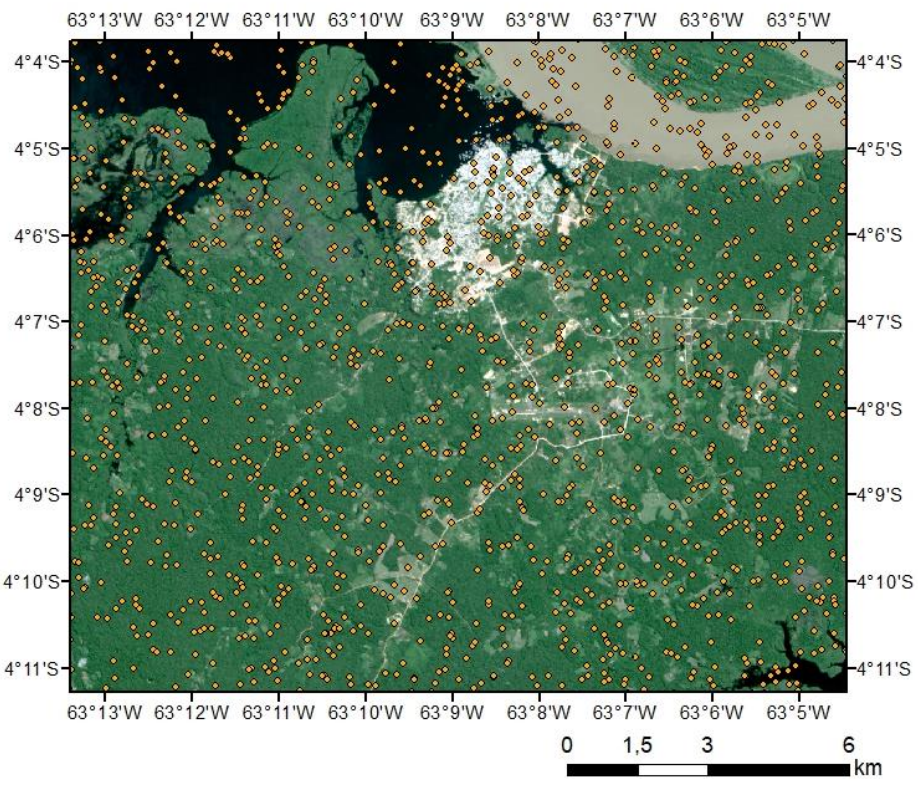


Figure 2 - Location of 1600 random points in the study area.

RESULTS AND DISCUSSION

Figures 3 and 4 present the maps of the classification of land cover, surface albedo, NDVI, NDBI, surface temperature (LST), and the difference between the surface temperature and the brightness temperature (LST-BT) in the respective dates of 2015 and 2017. The urbanized regions showed considerably higher surface albedo than densely vegetated areas, as presented in the NDVI map. The areas with high surface albedo values presented higher LST values, and regions with higher NDVI showed lower LST values. This indicates that, although urbanized regions have higher albedo, that is, greater capacity to reflect solar radiation, the small amount of water available on the surface for the evapotranspiration process (latent heat) prevails over the use of the energy available for heating (sensitive heat). In densely vegetated areas, despite solar radiation being absorbed in a much higher amount, LST is lower, which indicates that most of the available energy was used as latent heat. That is, to control the LST, the higher surface reflection coefficient of urban areas is less efficient than the greater availability of water on the vegetation surface. Jenks's natural intervals method (Jenks, 1967) was used in the usual classification of the intervals present in the legends of the last two maps. A relevant observation is a difference of nearly 3°C between the temperature of the dark and stationary water of Coari Lake and the flowing and muddy water of the Solimões River (Fig. 1).

Scatter plots (Fig. 5 and 6) allow a few conclusions in isolation. Although there is a clear tendency to reduce LST with the increase in NDVI and increase in LST with Albedo and NDBI, these relationships are not linear (low R² in general), but such a hypothesis cannot be completely ruled out at a level of significance of 0.05. The correlations between these pairs can be seen in Table 1, which illustrates the moderate negative correlation between LST NDVI $_{
m the}$ and moderate positive correlation between LST and Albedo and the strong positive correlation between LST and NDBI. This reinforces the superior role of increased water availability in vegetation in thermal control, compared to the surface reflection coefficient. It is noteworthy that these values were not sampled on bodies of water, as we understand that this would distort the results.

Figure 3 - Classification of soil cover, surface Albedo, NDVI, NDBI, surface temperature (LST - with the average temperatures of each region in parentheses) and the difference between surface temperature and brightness temperature (LST -BT) on 24/08/2015, at 10:25 (local time) in Coari, Amazonia, Brazil.

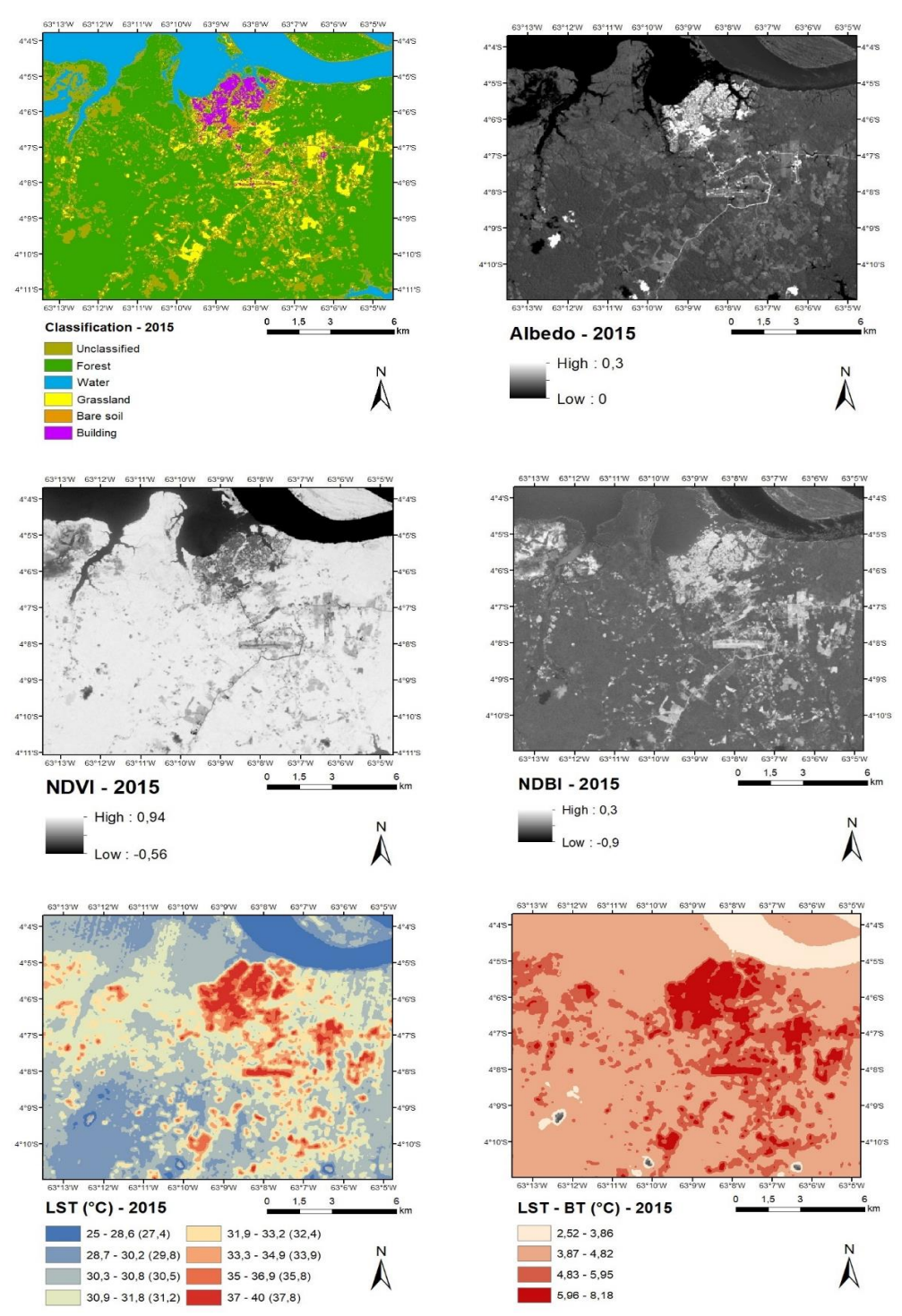
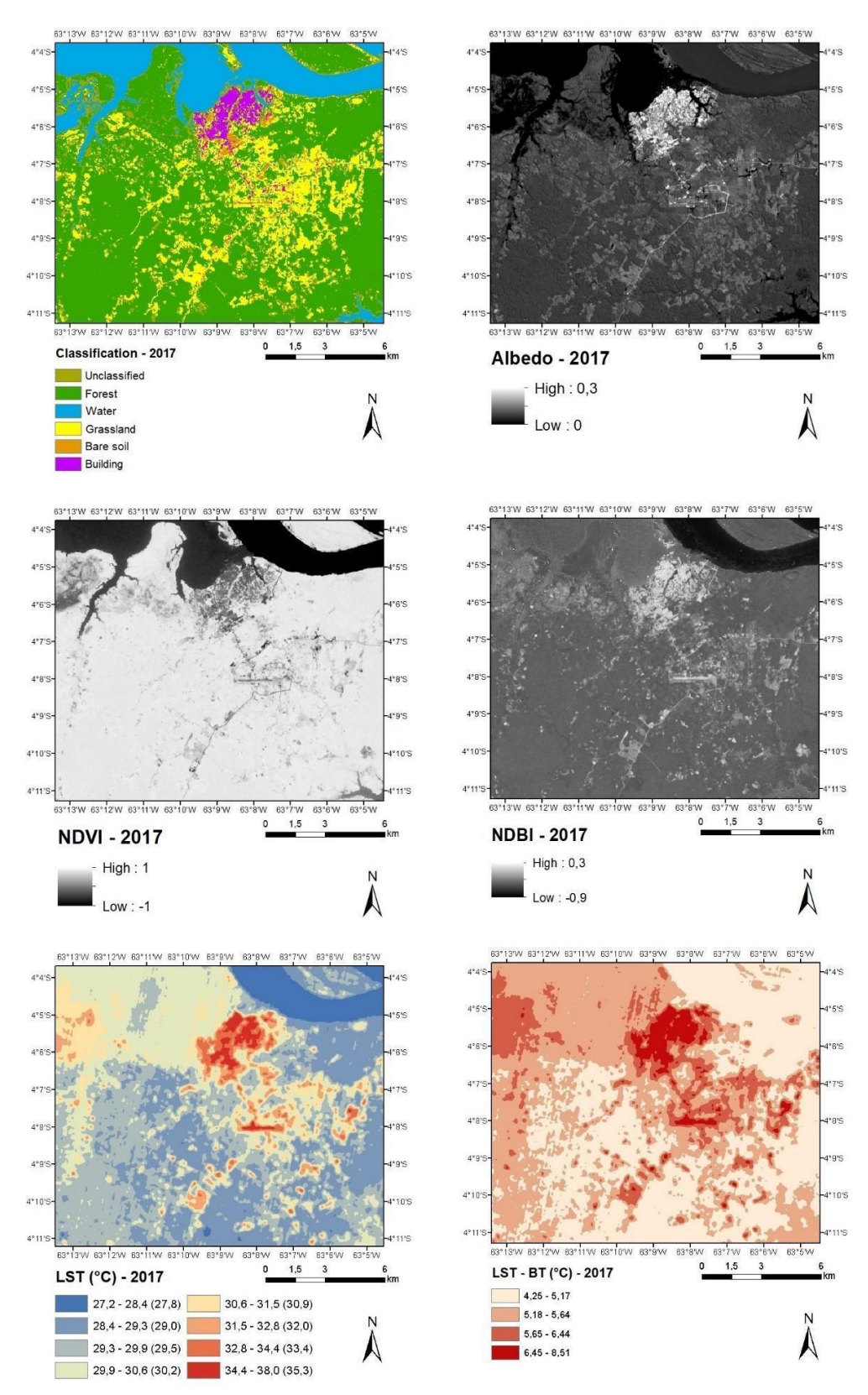


Figure 4 - Classification of soil cover, surface Albedo, NDVI, NDBI, surface temperature (LST - with average temperatures of each region in parentheses) and the difference between surface temperature and brightness temperature (LST -BT) on 26/06/2017, at 10:25 (local time) in Coari, Amazonia, Brazil.

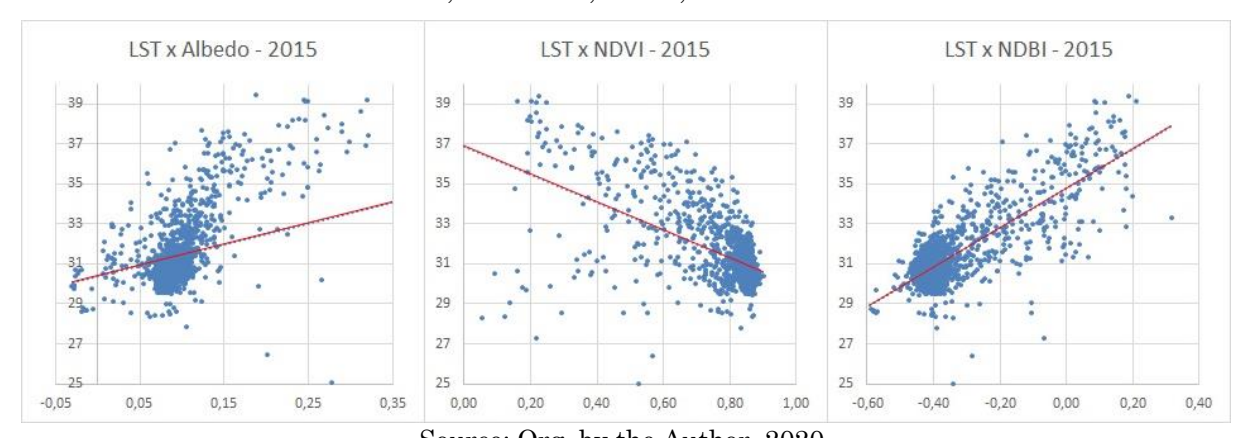


The effect of atmospheric correction on the surface temperature must also be evaluated. The most significant differences between LST and BT occurred in less vegetated regions, reaching 8°C. This shows how critical the use of atmospheric correction are performed.

To compare LST on the analyzed dates, the difference between temperatures in 2015 and 2017 (Fig. 7) was plotted. The LST in 2015 was higher than in 2017, except in water bodies. The higher values on bare soil in 2015 are

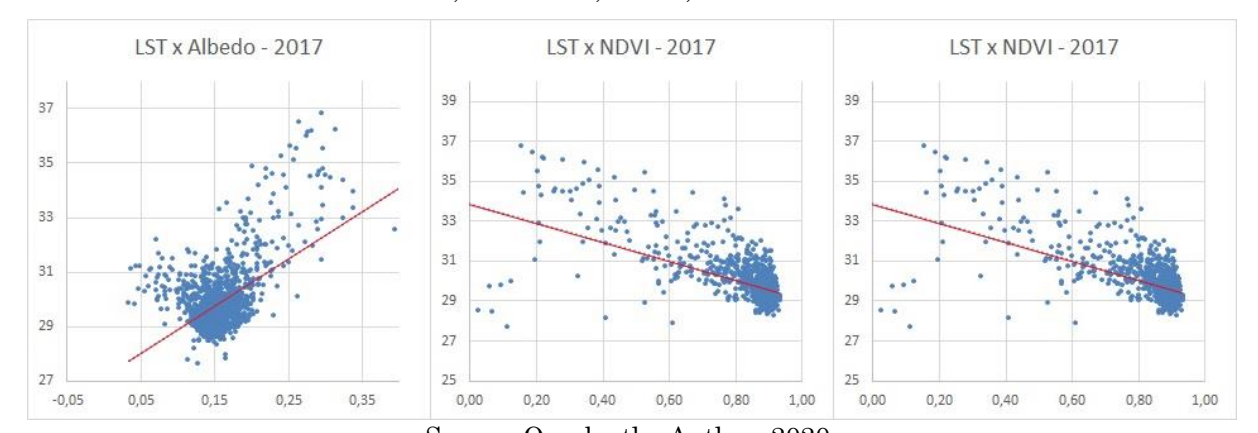
understandable, as August is the beginning of the so-called Amazonian summer (hot and dry), in addition to the exceptionally strong El Niño in 2015 (INPE, 2016). The lower LST in the bodies of water, on the other hand, are at least non-intuitive, as they coincide with an ebb period when temperatures should be increasing (SANTOS; RIBEIRO, 1988). This also suggests that there is little influence of the LST of water bodies on the LST of the adjacent bare soil regions.

Figure 5 - Scatter plots between surface temperature (LST), surface albedo, NDVI, and NDBI in Coari, Amazonas, Brazil, on 08/24/2015.



Source: Org. by the Author, 2020.

Figure 5 - Scatter plots between surface temperature (LST), surface albedo, NDVI, and NDBI in Coari, Amazonas, Brazil, on 26/06/2017.



Source: Org. by the Author, 2020.

Table 1 - Correlation coefficient (r) and determination coefficient (R²) between surface temperature (LST), surface albedo, NDVI, and NDBI in Coari, Amazonas, Brazil.

Data	Coefficient	LST x Albedo	LST x NDVI	LST x NDBI
24/08/2015	r	0,303	-0,550	0,761
	\mathbb{R}^2	0,092	0,303	0,579
16/06/2017	r	0,546	-0,595	0,755
	R^2	0,298	0,354	0,570

Source: Org. by the Author, 2020

63°12'W 63°11'W 63°10'W 63°8'W 63°5'W 4°4'S 4°4'S 4°6'5 4°6'S 4°7'S 4°7'S 4°8'S 4°8'S 4°9'S 4°9'S 4°10'S 4°10'S 4°11'S 63°12'W 63°11'W 63°10'W 63°9'W 63°8'W 1,5 LST(2015) - LST(2017) (°C) -2.96 - 0 0.01 - 1.31,31 - 2,33 2,34 - 3,91 3,92 - 7,94

Figure 7 - Difference between surface temperatures (LST) in Coari, Amazonas, Brazil, in 2015 and 2017. Except for a few clouds (and shadows), the only relevant regions that showed the coldest in 2015 are bodies of water.

FINAL CONSIDERATIONS

There was a considerable influence of vegetation in controlling surface temperature, even in urbanized areas, than the surface reflection coefficient (surface albedo). Urbanized regions had surface temperatures up to 7°C higher than densely vegetated areas.

The atmospheric correction of the surface temperature is essential in urbanized areas, as the values can be underestimated by 4 to 7°C without its application. The surface temperature in 2015 was substantially higher on bare soil regions, but lower on bodies of water.

Finally, this study shows the importance of afforestation and vegetation in urban centers, especially in the hot areas, as is the case in the western Amazon.

REFERENCES

AB'SABER, A. N. Zoneamento fisiográfico e ecológico do espaço total da Amazônia Brasileira. **Estud. av.**, São Paulo, v. 24, n. 68, p. 15-24, 2010. https://doi.org/10.1590/S010340142010000100 004

ALHAWITI, R. H.; MITSOVA, D. Using Landsat-8 data to explore the correlation between Urban Heat Island and Urban Land uses. International Journal of Research in Engineering and Technology. V. 5, p. 457-466, 2016. https://doi.org/10.15623/ijret.2016.0503083

ALLEN, R. G.; TASUMI, M.; TREZZA, R. Satellite-based energy balance for mapping evapotranspiration with internalized calibration (METRIC) – Model. **Journal of Irrigation and Drainage Engineering.** V.133, n.4, p. 380- 394, 2007. https://doi.org/10.1061/(ASCE)07339437(2007) 133:4(380)

- BARSI, J.A.; BARKER, J.L.; SCHOTT J.R. An Atmospheric Correction Parameter Calculator for a Single Thermal Band Earth-Sensing Instrument. **Geoscience and Remote Sensing Symposium** (Anals), Centre de Congres Pierre Baudis, Toulouse, France, 2003.
- BIUDES, M.S.; VOULITIS, G.L.; MACHADO, N.G.; DE ARRUDA, P.H.Z.; NEVES, G.A.R.; LOBO, F.A.; NEALE, C.M.U.; NOGUEIRA, J.S. Patterns of energy exchange for tropical ecosystems across a climate gradiente in Mato Grosso, Brazil. **Agricultural and Forest Meteorology**, v. 202, p. 112–124, 2015. https://doi.org/10.1016/j.agrformet.2014.12.00
- CARLSON, T.; RIPLEY, D. A. On the relation between NDVI, fractional vegetation cover, and leaf area index. **Remote Sensing of Environment**. V. 62, p. 241-252, 1997. https://doi.org/10.1016/S0034-4257(97)00104-1
- CHEN, X.; ZHAO, H; LI, P.; YIN, Z. Remote sensing image-based analysis of the relationship between urban heat island and land use/cover changes, **Remote Sensing of Environment**, V. 104, Issue 2, P. 133-146, 2006. ISSN 0034-4257. https://doi.org/10.1016/j.rse.2005.11.016
- DARCAN, N.; GÜNEY, O. Alleviation of climatic stress of dairy goats in Mediterranean climate. **Small Ruminant Research.** Vol.74, 212-215, 2008. https://doi.org/10.1016/j.smallrumres.2007.02.007
- ESPA EROS Science Processing Architecture On Demand Interface. 2019. Disponível em https://espa.cr.usgs.gov/>
- FEARNSIDE, P. M. Desmatamento na Amazônia: dinâmica, impactos e controle. Acta Amazônica, v. 36(3), p. 395 400, 2006. https://doi.org/10.1590/S0044-59672006000300018
- FERREIRA, L. V.; VENTICINQUE, E.; ALMEIDA, S. O desmatamento na Amazônia e a importância das áreas protegidas. **Estud. av.**, São Paulo, v. 19, n. 53, p. 157-166, 2005. https://doi.org/10.1590/S010340142005000100 010
- GAOUA, N.; RACINAIS, S.; GRANTHAM, J.; EL MASSIOUI, F. Alterations in cognitive performance during passive hyperthermia are task dependent. **Int. J. Hyperthermia** 27, 1–9 (2011) https://doi.org/10.3109/02656736.2010.516305
- GARTLAND, L. Ilhas de calor: como mitigar zonas de calor em áreas urbanas. São Paulo: Oficina de Textos, 2010.

- GLOVIS Global Visualization Viewer. The USGS Global Visualization Viewer (GloVis). 2019. Disponível em https://glovis.usgs.gov/>.
- GSFC NASA's Goddard Space Flight Center. **Atmospheric Correction Parameter Calculator.** 2019. Disponível em https://atmcorr.gsfc.nasa.gov/>.
- GUILHERME, A. P. et al. USO DE ÍNDICE DE VEGETAÇÃO PARA CARACTERIZAR A MUDANÇA NO USO DO SOLO EM COARIAM. Soc. nat., Uberlândia, v. 28, n. 2, p. 301-310, ago. 2016. http://dx.doi.org/10.1590/1982-451320160209.
- INSTITUTO BRASILEIRO DE GEOGRAFIA E ESTATÍSTICA IBGE [Brazilian Institute of Geography and Statistics]. Available in http://cidades.ibge.gov.br/painel/painel.php?codmun=130120. 2011
- INSTITUTO NACIONAL DE PESQUISAS ESPACIAIS/ CENTRO DE PREVISÃO DE TEMPO E ESTUDOS CLIMÁTICOS [NATIONAL SPACE RESEARCH INSTITUTE Brazil]. Impactos do fenômeno ENOS, 2016. Available in: http://enos.cptec.inpe.br>. Acesso em 23 dez. 2016.
- JENKS, G. F. The Data Model Concept in Statistical Mapping. **International Yearbook of Cartography**. V. 7, P. 186– 190, 1967.
- MADER T.L.; JOHNSON L.J.; GAUGHAN, J.B. A comprehensive index for assessing environmental stress in animals. **Journal of Animal Science.** Vol. 88, 2153-2165, 2010. https://doi.org/10.2527/jas.2009-2586
- MCMORRIS, T. et al. Heat stress, plasma concentrations of adrenaline, noradrenaline, 5-hydroxytryptamine and cortisol, mood state and cognitive performance. Int. J. Psychophysiol. 61, 204-215 (2006). https://doi.org/10.1016/j.ijpsycho.2005.10.002
- MEDEIROS, S.S.; CECÍLIO, R.A.; MELO JÚNIOR, J.C.F. Estimativa e espacialização das temperaturas do ar mínimas, médias e máximas na Região Nordeste do Brasil. Revista Brasileira de Engenharia Agrícola e Ambiental, v. 9, n. 2, p. 247-255, 2005. https://doi.org/10.1590/S1415-43662005000200016
- MOURÃO, G. M. N. Colonización reciente y asentamientos rurales en el sureste de Roraima, Amazonia Brasileña: entre la política y la naturaleza. 2003. 480f. Doctoral thesis, Universidad de Valladolid, Espanha. 2003.
- PAVAO, V. M. et al. Impacto da Conversão da Cobertura Natural em Pastagem e Área

- Urbana sobre Variáveis Biofísicas no Sul do Amazonas. **Rev. bras. meteorol.** V. 32, n. 3, p. 343-351, 2017. http://dx.doi.org/10.1590/0102-77863230002.
- PRICE, J. C. Estimating surface temperatures from satellite thermal infrared data a simple formulation for the atmospheric effect. **Remote Sens. Environ**. V. 13, p. 353-361, 1983.https://doi.org/10.1016/00344257(83)900 36-6
- SANTOS, U. M.; RIBEIRO, M. N. G. A hidroquímica do Rio Solimões Amazonas. **Acta Amaz.** Manaus, v. 18, n. 3-4, p. 145-172, 1988 https://doi.org/10.1590/18094392198818 3172
- SHALABY, A. E.; TATEISHI, R. Remote sensing and GIS for mapping and monitoring land cover and land-use changes in the Northwestern coastal zone of Egypt, **Applied Geography**, V. 27, Issue 1, 2007, Pages 28-41, ISSN 0143-6228. https://doi.org/10.1016/j.apgeog.2006.09.004
- SILVA, B. B.; BRAGA, A. C.; BRAGA, C. C.; OLIVEIRA, L. M. M.; MONTENEGRO, S. M. G. L.; BARBOSA JUNIOR, B. Procedures for calculation of the albedo with OLI-Landsat 8 images: Application to the Brazilian semi-arid. Revista Brasileira de Engenharia Agrícola e Ambiental. v.20, n.1, p.3–8, 2016.http://dx.doi.org/10.1590/18071929/agria mbi.v20n1p3-8
- STERN, N. The structure of economic modeling of the potential impacts of climate change: Grafting gross underestimation of risk onto already narrow science models. **J. Econ. Lit.** 51, 838–859 (2013). https://doi.org/10.1257/jel.51.3.838
- TAMM, M. *et al.* The compression of perceived time in a hot environment depends on physiological and psychological factors. **Q. J. Exp. Psychol.** 67, 197–208 (2014). https://doi.org/10.1080/17470218.2013.804849
- TAWATSUPA, B. *et al.* Association between heat stress and occupational injury among Thai workers: Findings of the Thai cohort study. **Ind. Health** 51, 34–46 (2013). https://doi.org/10.2486/indhealth.2012-0138
- TUCKER, C. J. Red and photographic infrared linear combinations for monitoring vegetation. **Remote Sens. Environ**. V. 8, P. 127–150. 1979 https://doi.org/10.1016/0034-4257(79)90013-0
- USGS United States Geological Survey. **Landsat 8 Data Users Handbook.** Digital edition. Version 2.0. 2016. Available in
- https://landsat.usgs.gov/sites/default/files/documents/Landsat8DataUsersHandbook.pdf.

- VALOR, E.; CASELLES Vicente. Mapping Land Surface Emissivity from NDVI: Application to European, African, and South American Areas. **Remote Sensing of Environment.** V. 57, p. 167-184. 1996. https://doi.org/10.1016/0034-4257(96)00039-9
- VAREJÃO-SILVA, M.A. **Meteorologia e Climatologia**. Digital version 2. Recife, PB, 2006, 463p.
- ZANDER, K. K. et al. Heat stress causes substantial labour productivity loss in Australia. Nature Climate Change. v. 5, pages 647–651 (2015). https://doi.org/10.1038/nclimate2623